Investigation of a method to calculate spontaneous radiation spectra from relativistic electrons in undulators

CHEN Ming-Zhi(陈鸣之) HE Jian-Hua(何建华)[1)]

(Shanghai Institute of Applied Physics, Chinese Academy of Sciences, Shanghai 201800，China)

Abstract Undulators are key devices to produce brilliant synchrotron radiation at the synchrotron radiation facilities. In this paper we present a numerical computing method, including the computing program that has been developed to calculate the spontaneous radiation emitted from relativistic electrons in undulators by simulating the electrons' trajectory. The effects of electron beam emittance and energy spread have also been taken into account. Comparing with other computing methods available at present, this method has a few advantages with respect to several aspects. It can adopt any measured or arbitrarily simulated 3D magnetic field and arbitrary electron beam pattern for the calculation and it's able to analyze undulators of any type of magnetic structure. It's expected to predict precisely the practical radiation spectrum. The calculation results of a short period in-vacuum undulator and an Elliptically Polarized Undulator (EPU) at Shanghai Synchrotron Radiation Facility (SSRF) are presented as examples.

Key words undulator, spontaneous radiation, electron trajectory, Runge-Kutta method

PACS 41.60.Ap, 07.85.Qe

1 Introduction

Synchrotron Radiation (SR) has become a very powerful tool for the researches in many fields since the 1990s[1]. Undulators, which consist of periodic magnetic arrays and can produce brilliant synchrotron radiation, have been widely used at the 3rd generation SR facilities. When relativistic electrons pass through the periodic magnetic field of an undulator, they oscillate in the transverse direction and emit partly coherent electromagnetic radiation. Due to the interference of radiation in different periods, the undulator radiation becomes quasi-monochromatic and its brightness is greatly enhanced.

In the last thirty years, the theory of undulator radiation has been well developed and several methods to calculate the spectrum of undulator radiation have been established[2—8]. A few computing codes based on those methods, such as SPECTRA[3], XOP[4—7] and SRW[8], have been created to understand the properties of undulator radiation and to help the design of undulators. Some of them use directly the theoretical formulae for the calculation (XOP), and some others (e.g. SPECTRA) simulate the electron trajectory and have more accurate results. There were also continuous efforts done by a few research groups in China[9—14]. These activities included the software development for the calculation of radiation distribution produced by one-dimensional linearly polarized magnetic fields[9], the numerical simulation and a simulation code to investigate the influence of emittance, energy spread, off-axis and oblique axis on the spontaneous emission spectra in the Optical Klystron of NSRL[11] and the simulation study of the influence of magnetic field errors on the undulator radiation[14]. Meanwhile, the manufacturing technology of undulators made also great progress. Mini-gap undulators have been widely used to produce brilliant high harmonics radiation, and undulators with various magnetic structures have been designed to produce the desired features of radiation. It is becoming feasible to fabricate the undulator with very small magnetic errors, so to achieve the performance as designed. This also enhanced the request for a precise calculation of the undulator radiation specific to various experimental demands. The existing computing codes

Received 4 January 2008

1) E-mail: hejh@sinap.ac.cn

are not sufficient for the calculation of undulator radiation with any magnetic structures, which would be useful for evaluating the effect of magnetic field errors on the undulator radiation.

In this paper, we propose a computing method aiming at the precise calculation of the undulator radiation spectrum. The related computing program, named Undulator Radiation Computing Program (URCP), is based on electrodynamics[15] and can adopt any 3D magnetic fields in the calculation. Different from other computing codes, such as SPECTRA and XOP, the Variation of the Magnet field intensity in the Transverse direction (VMT) has been taken into account in URCP. VMT can affect seriously the undulator radiation in certain situations. To illustrate the usage of URCP, two types of undulators used at SSRF have been taken as the calculation examples and their results are compared with those of other codes.

2 Basic theory and calculation method

2.1 Single electron radiation

According to the theory of electrodynamics, an electron emits an electromagnetic wave while it is accelerated. The equations of the radiation field can be expressed as:

$$\begin{aligned}\boldsymbol{E}(x,t) = & \frac{e}{4\pi\varepsilon_0 cR}\left\{\frac{\boldsymbol{n}-\boldsymbol{\beta}}{\gamma^2(1-\boldsymbol{\beta}\cdot\boldsymbol{n})^3R^2}+\right.\\ & \left.\frac{\boldsymbol{n}\times\left[(\boldsymbol{n}-\boldsymbol{\beta})\times\dfrac{\mathrm{d}\boldsymbol{\beta}}{\mathrm{d}t}\right]}{(1-\boldsymbol{n}\cdot\boldsymbol{\beta})^3}\right\}^*, \qquad (1)\\ \boldsymbol{B} = & \frac{1}{c}\times\boldsymbol{n}\times\boldsymbol{E},\end{aligned}$$

where ε_0, c, e, $\boldsymbol{\beta}$, R, $\boldsymbol{n}$ are the permittivity of the vacuum, the light velocity in vacuum, the charge of the electron, the relative velocity of the moving electron, the distance from electron to the observation position, and the unit vector from the electron to the observation position, respectively. The symbol * means that retarded form has to be taken.

Then, the single electron radiation power density per unit solid angle is given by the equation:

$$\begin{aligned}\frac{\mathrm{d}P}{\mathrm{d}\Omega} = & \varepsilon_0 c\int_{-\infty}^{\infty}|E(t)|^2\mathrm{d}t = \frac{e^2\gamma^4}{2\pi^2\varepsilon_0^2c^2}\times\\ & \int_{-\infty}^{\infty}\left[\frac{(\gamma\dot{\beta}_x)^2+(\gamma\dot{\beta}_y)^2}{D^3}-\right.\\ & \left.\frac{4(\xi\gamma\dot{\beta}_x+\psi\gamma\dot{\beta}_y)^2}{D^5}+\frac{4c^2(\xi^2+\psi^2)}{R^2D^5}\right]^2\frac{\mathrm{d}t'}{R^2}, \qquad (2)\end{aligned}$$

with

$$\begin{aligned}D = & 1+\xi^2+\psi^2,\\ \xi = & \gamma n_x-\gamma\beta_x,\\ \psi = & \gamma n_y-\gamma\beta_y, \qquad (3)\\ t' = & t-\frac{R}{c},\\ \gamma = & E_\mathrm{e}/mc^2.\end{aligned}$$

The Fourier transform of the Electric field intensity can be written as:

$$\begin{aligned}E(t) = & \int_{-\infty}^{\infty}E(\omega)\exp(-\mathrm{i}\omega t)\mathrm{d}\omega,\\ E(\omega) = & \frac{1}{2\pi}\int_{-\infty}^{\infty}E(t)\exp(\mathrm{i}\omega t)\mathrm{d}t.\end{aligned} \qquad (4)$$

Then we can obtain the total radiation power per unit solid angle by integrating over t in Eq. (2):

$$\begin{aligned}\frac{\mathrm{d}I}{\mathrm{d}\Omega} = & \int_{-\infty}^{\infty}\frac{\mathrm{d}P(t)}{\mathrm{d}\Omega}\mathrm{d}t = \varepsilon_0 cR^2\int_{-\infty}^{\infty}[E^2]^*\,\mathrm{d}t = \\ & 4\pi\varepsilon_0 cR^2\int_0^{\infty}|E(\omega)|^2\mathrm{d}\omega\ . \qquad (5)\end{aligned}$$

Taking the derivatives with respect to ω on both sides, we have:

$$\frac{\mathrm{d}^2I}{\mathrm{d}\omega\mathrm{d}\Omega} = 4\pi\varepsilon_0 cR^2\,|E(\omega)|^2\ . \qquad (6)$$

If R is much longer than the undulator length, we can apply the far-field approximation to simplify the equation of radiation intensity per unit solid angle:

$$\begin{aligned}\frac{\mathrm{d}^2I}{\mathrm{d}\omega\mathrm{d}\Omega} = & \frac{e^2\omega^2}{16\pi^3c}\left|\int_{-\infty}^{+\infty}\boldsymbol{n}\times(\boldsymbol{n}\times\boldsymbol{\beta})\times\right.\\ & \left.\exp\left[+\mathrm{i}\omega\left(\frac{t'-\boldsymbol{n}\times\boldsymbol{r}(t')}{c}\right)\right]\mathrm{d}t'\right|^2. \qquad (7)\end{aligned}$$

Most of the radiation characteristics can be calculated by using Eq. (2) and (7).

2.2 The effect of multi-electrons

In the storage ring of synchrotrons, electrons are confined into separate electron bunches. Fig. 1 shows the coordirate system of the j-th electron in an eletron bunch. By using Eq. (7), the radiation spectrum generated by an electron bunch with N_e electrons can be written as:

$$\begin{aligned}\left.\frac{\mathrm{d}^2I}{\mathrm{d}\omega\mathrm{d}\Omega}\right|_{N_\mathrm{e}e} = & \frac{e^2\omega^2}{16\pi^3c}\left|\sum_{j=1}^{N_\mathrm{e}}\int_{-\infty}^{+\infty}\boldsymbol{n}\times(\boldsymbol{n}\times\boldsymbol{\beta}_j)\times\right.\\ & \left.\exp[+\mathrm{i}\omega(t'-\boldsymbol{n}\times\boldsymbol{r}(t')/c)]\mathrm{d}t'\right|^2, \qquad (8)\end{aligned}$$

where $\boldsymbol{\beta}_j$ and $\boldsymbol{R}_j(t)$ are the velocity and position vector of the j-th electron at time t, respectively.

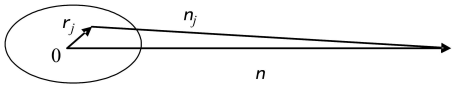

Fig. 1. Scheme of the effect of multi-electrons.

In principle, the interferential effects of radiation generated from different electrons are taken into account by this equation. However, the electrons in an electron bunch are not confined tight enough to cause observable interference effect of X-rays emitted from different electrons. Therefore the radiation intensity of an electron bunch can be calculated by adding together the radiation intensity of each electron inside the electron bunch:

$$\left.\frac{\mathrm{d}^2I}{\mathrm{d}\omega\mathrm{d}\Omega}\right|_{\mathrm{inc}}=\sum_{j=1}^{N_{\mathrm{e}}}\left.\frac{\mathrm{d}^2I}{\mathrm{d}\omega\mathrm{d}\Omega}\right|_{j}. \tag{9}$$

3 Numerical computing method

Given the parameters of a particle's velocity and trajectory, the radiation power density and spectrum can be obtained through Eq. (2) and (7).

The equation of motion for an electron in an electromagnetic field can be expressed as:

$$\frac{\mathrm{d}^2\boldsymbol{R}(t')}{\mathrm{d}t^2}=-\frac{e}{\gamma m}\left(\boldsymbol{E}_{\mathrm{f}}+\boldsymbol{B}\times\boldsymbol{v}(t')\right), \tag{10}$$

where $\boldsymbol{E}_{\mathrm{f}}$, $\boldsymbol{B}$, $\boldsymbol{R}(t')$ and $\boldsymbol{v}(t')$ are external electric field strength, external magnetic field strength, the electron position and the electron velocity at time t', respectively.

Considering $\boldsymbol{v}(t')=\dfrac{\mathrm{d}\boldsymbol{R}(t')}{\mathrm{d}t}$ and letting $\dfrac{\mathrm{d}\boldsymbol{v}(t')}{\mathrm{d}t}=f(t',\boldsymbol{R},\boldsymbol{v})$, we can derive the following equations from Eq. (10) through the Runge-Kutta method[16]:

$$\begin{cases}\boldsymbol{R}_{j+1}=\boldsymbol{R}_{j+1}+\boldsymbol{v}\Delta t+\dfrac{\Delta t^2}{6}(\boldsymbol{l}_1+\boldsymbol{l}_2+\boldsymbol{l}_3),\\ \boldsymbol{v}_{j+1}=\boldsymbol{v}_j+\dfrac{\Delta t}{6}(\boldsymbol{l}_1+2\boldsymbol{l}_2+2\boldsymbol{l}_3+\boldsymbol{l}_4),\end{cases} \tag{11}$$

with

$$\begin{cases}\boldsymbol{l}_1=f(t'_j,\boldsymbol{R}_j,\boldsymbol{v}_j),\\ \boldsymbol{l}_2=f\left(t'_j+\dfrac{\Delta t'}{2},\boldsymbol{R}_j+\dfrac{\Delta t'}{2}\boldsymbol{v}_j,\boldsymbol{v}_j+\dfrac{\Delta t'}{2}\boldsymbol{l}_1\right),\\ \boldsymbol{l}_3=f\left(t'_j+\dfrac{\Delta t'}{2},\boldsymbol{R}_j+\dfrac{\Delta t'}{2}\boldsymbol{v}_j+\dfrac{\Delta t'^2}{4}\boldsymbol{l}_1,\boldsymbol{v}_j+\dfrac{\Delta t'}{2}\boldsymbol{l}_2\right),\\ \boldsymbol{l}_4=f\left(t'_j+\Delta t',\boldsymbol{R}_j+\Delta t'\boldsymbol{v}_j+\dfrac{\Delta t'^2}{2}\boldsymbol{l}_2,\boldsymbol{v}_j+\Delta t'\boldsymbol{l}_3\right).\end{cases} \tag{12}$$

Given the initial electron position $\boldsymbol{R}(0)$ and velocity $\boldsymbol{v}(0)$, the electron trajectory and velocity can be derived from Eq. (12) with the parameters of the undulator magnetic field.

For numerical computing, Eq. (2) and (7) are transformed into discrete equation:

$$\begin{aligned}\frac{\mathrm{d}P}{\mathrm{d}\Omega}=&\int_{-\infty}^{\infty}\left[\frac{(\gamma\dot{\beta}_x)^2+(\gamma\dot{\beta}_y)^2}{D^3}-\frac{4(\xi\gamma\dot{\beta}_x+\psi\gamma\dot{\beta}_y)^2}{D^5}+\right.\\ &\left.\frac{4c^2(\mathrm{d}\xi^2+\psi^2)}{R^2D^5}\right]\frac{\mathrm{d}t'}{R^2}=\\ &\frac{e^2\gamma^4}{2\pi^2\varepsilon_0^2c^2}\sum_{j=1}^{N}\left[\left(\frac{P_1(j)}{D[j]^3}-\frac{P_2(j)}{D[j]^5}+\frac{P_3(j)}{R^2D[j]^5}\right)\times\right.\\ &\left.(t'[j]-t'[j-1])\right],\end{aligned} \tag{13}$$

with

$$\begin{aligned}P_1[j]=&\ \gamma^2\left(\dot{\beta}_x[j]^2+\dot{\beta}_y[j]^2\right),\\ P_2[j]=&\ 4\gamma^2\left[\left(\xi[j]\dot{\beta}_x[j]\right)^2+\left(\Psi[j]\dot{\beta}_y[j]\right)^2\right],\\ P_3[j]=&\ 4c^2(\xi[j]^2+\psi[j]^2),\\ D[j]=&\ 1+\xi[j]^2+\psi[j]^2,\\ \xi[j]=&\ \gamma n_x-\gamma\beta_x[j],\\ \psi[j]=&\ \gamma n_y-\gamma\beta_y[j],\end{aligned} \tag{14}$$

and

$$\begin{aligned}\frac{\mathrm{d}^2I}{\mathrm{d}\omega\mathrm{d}\Omega}=&\frac{e^2\omega^2}{16\pi^3c}\left|\int_{-\infty}^{+\infty}\boldsymbol{n}\times(\boldsymbol{n}\times\boldsymbol{\beta})\times\right.\\ &\left.\exp[+\mathrm{i}\omega(t'-\boldsymbol{n}\times\boldsymbol{r}(t')/c)]\mathrm{d}t'\right|^2=\\ &\frac{e^2\omega^2}{16\pi^3c}\sum_{k=1}^{3}\left\{\left[\sum_{j=2}^{N}F_k[j]\cos(FF[j])(t'[j]-t'[j-1])\right]^2+\right.\\ &\left.\left[\sum_{j=2}^{N}F_k[j]\sin(FF[j])(t'[j]-t'[j-1])\right]^2\right\},\end{aligned} \tag{15}$$

with

$$\begin{aligned}F_1[j]=&\ \sin^2\theta\cdot\cos^2\varphi\cdot\beta_x[j]+\sin^2\theta\cdot\sin\varphi\cdot\cos\varphi\cdot\beta_y[j]+\\ &\sin\theta\cdot\cos\theta\cdot\cos\varphi\cdot\beta_z[j]-\beta_x[j],\\ F_2[j]=&\ \sin^2\theta\cdot\sin\varphi\cdot\cos\varphi\cdot\beta_x[j]+\sin^2\theta\cdot\sin^2\varphi\cdot\beta_y[j]+\\ &\sin\theta\cdot\cos\theta\cdot\sin\varphi\cdot\beta_z[j]-\beta_y[j],\\ F_3[j]=&\ \sin\theta\cdot\cos\theta\cdot\cos\varphi\cdot\beta_x[j]+\\ &\sin\theta\cdot\cos\theta\cdot\sin\varphi\cdot\beta_y[j]+\cos^2\theta\beta_z[j]-\beta_z[j],\end{aligned}$$

$$\begin{aligned}FF[j]=&\ \omega\left[t'[j]-\right.\\ &\left.\frac{(\sin\theta\cdot\cos\varphi\cdot x[j]+\sin\theta\cdot\sin\varphi\cdot y[j]+\cos\varphi\cdot z[j])}{c}\right].\end{aligned} \tag{16}$$

Then we can get the radiation intensity of a single electron per unit solid angle and unit frequency by using the electron motion trajectory and velocity derived from Eq. (11) and (12). As Eq. (11) and (12) can adopt arbitrary 3D magnetic field data, this numerical method can adopt an arbitrary 3D magnetic field.

For an accurate calculation, the effect of multi-electrons in an electron bunch has to be taken into account. Since the number of electrons in an electron bunch is enormous, the Monte Carlo method is used to deal with the effect of an electron bunch:

$$\left.\frac{\mathrm{d}^2 I}{\mathrm{d}\omega \mathrm{d}\Omega}\right|_{N_\mathrm{e}} = \sum_{j=1}^{M} w_j \left.\frac{\mathrm{d}^2 I}{\mathrm{d}\omega \mathrm{d}\Omega}\right|_j , \qquad (17)$$

where w_j is the weight factor of the j-th electron, which depends on the initial parameter of the j-th electron and the distribution functions of both, the electron beam energy spread and the emittance. Given the initial parameters, the radiation intensity of different electron bunch patterns can be derived from Eq. (17).

4 Computing program

Based on the numerical computing method discussed above, the computing program URCP has been written in Visual C++ 6.0. For convenience, URCP has preset electron bunch data of Gaussian pattern and magnetic field data of ideal undulators, such as a conventional undulator, a helical undulator, EPU. The data for an arbitrary magnetic field and the electron bunch pattern have to be written into data files in a prescribed form as input into the URCP calculation.

Numerical computing will introduce truncation errors into the calculation. In the URCP we try to make the truncation errors negligible.

The key point is to calculate the phase term $FF[j]$ in Eq. (16) accurately. Assuming the rms errors of $FF[j]$ is ΔFF, the variation of the radiation intensity caused by ΔFF can be estimated by[19]:

$$I = I_0 \exp(-\Delta FF^2) . \qquad (18)$$

To keep the calculation error of the radiation intensity less than 1%, the calculation error of ΔFF must be less than 0.1. In the case of X-rays, the orders of magnitude of ω and t are generally between 10^{17}—10^{20} and 10^{-9}—10^{-8} s, respectively, so the precision of t and R should be up to 10^{-14} s and 10^{-10}—10^{-13} m, respectively. Thus, an accurate calculation of the electron trajectory is requested. URCP uses a fourth order Runge-Kutta method. While the step length takes 10^{-4} m, the local truncation error would be less than 10^{-20}. In this way the URCP meets the demand mentioned before, even for the calculation of very high order of harmonics.

5 Examples calculated with URCP

A few typical examples have been taken to illustrate the usage and the function of the URCP. In the calculation hereafter, unless specified explicitly, the parameters of the electron beam was taken from the designed parameters of the SSRF storage ring (Table 1).

Table 1. Parameters of the SSRF storage ring.

energy	current	natural emittance (mode 1)	natural emittance (mode 2)	coupling constant	β_x, β_y, η_x in middle of 6.5 m straight	energy spread
3.5 GeV	300 mA	3.9 nm·rad	11.2 nm·rad	$\leqslant$0.01	3.6, 2.5, 0.11 m	0.0097

5.1 Typical undulator with ideal magnetic field

A short period planar undulator is typically used to produce a brilliant SR beam at various harmonics to cover a wide photon energy range. The magnetic field of a planar undulator usually lies in the vertical direction (y- direction) and varies periodically along the longitudinal direction (z- direction). Fig. 2 shows the radiation spectrum of a planar undulator (U25) which has 80 periods with a period length of 25 mm. The magnetic field is assumed as an ideal magnetic field with K=2.2565 (deflection parameter). In this figure, the peak intensity decreases obviously and the peak position slightly shifts to the low energy side due to the effect of beam emittance and energy spread.

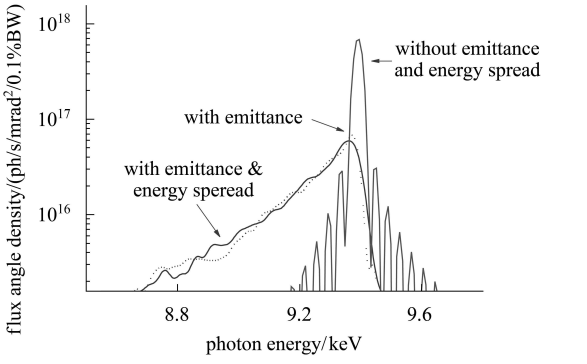

Fig. 2. Radiation spectrum of U25 (K=2.2565, the 3-rd harmonic).

Some experiments, such as energy dispersive techniques and extended X-ray absorption fine structure,

prefer a broad bandwidth and fast energy turning. For this purpose, U25 can be operated on tapered mode to satisfy these requirements. Fig. 3 shows the tapered mode of U25.

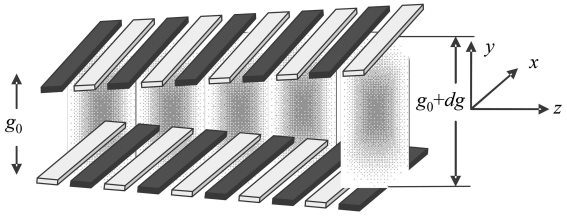

Fig. 3. Scheme of a tapered undulator.

The gap is assumed to be linearly tapered:

$$g(z) = g_0 + \frac{dg}{L}z \ , \tag{19}$$

Where dg, L, z are the difference of the entrance and exit magnetic gaps, undulator length, and the coordinate along the undulator, respectively.

Then the relationship between the peak magnetic field intensity B_0 and z can be approximately expressed as[20]:

$$B_0(z) = 2.983\exp\left[-\frac{g(z)}{\lambda_u}\left(5.068 - 1.52\frac{g(z)}{\lambda_u}\right)\right], \tag{20}$$

where λ_u is the period length.

The magnetic field distribution can be simply expressed as:

$$B_y = B_0(z)\sin\left(\frac{2\pi}{\lambda_u}z\right). \tag{21}$$

Figure 4 is the simulation results of U25 under tapered mode.

Figure 4 shows the on-axis flux angle density spectra calculated by means of URCP and SPECTRA with parameters shown under the figure. It is found that the bandwidth becomes broader while increasing the taper[7]. As shown in the figure, the difference between the results calculated by the two programs is less than 3%. Fig. 5 shows the comparison of the radiation spectra of U25 under planar mode calculated by URCP and SPECTRA.

In the comparison, the same parameters have been used and the Gaussian distribution beam pattern has been adopted. The calculated curves match well with each other. The difference of the peak flux density given by the two programs is less than 3% and the exact values are shown in Table 2. The minor difference could be attributed to the different ways in treating the electron beam emittance and energy spread[17]. The URCP uses a Monte Carlo method to simulate the electron beam, while SPECTRA uses a convolution of the flux intensity with a distribution function.

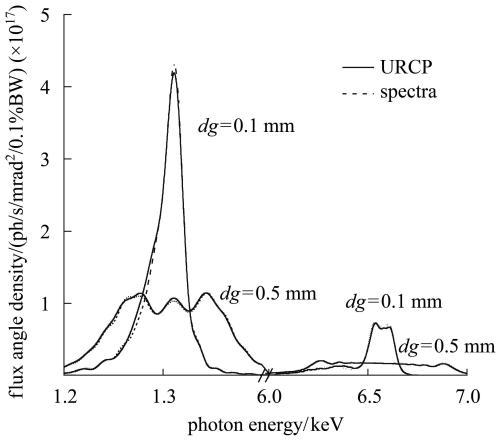

Fig. 4. Centre flux angle density with different tapers (g_0=6 mm, dg=0.1, 0.5 mm).

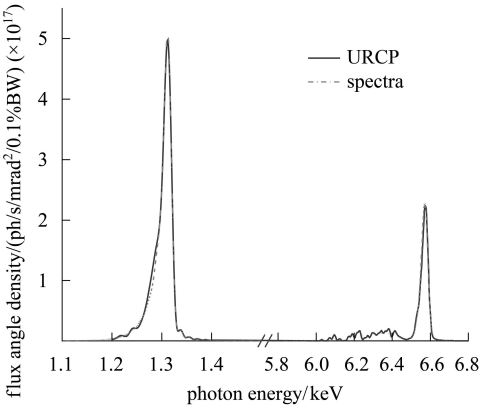

Fig. 5. Radiation spectra calculated by URCP and SPECTRA (U25 under planar mode).

In addition the URCP can adopt other electron beam patterns, such as a uniform distribution pattern, or add random noise to the patterns.

5.2 Undulator with quasi-arbitrary magnetic field

Quasi-arbitrary magnetic field here means that all

Table 2. Comparisons between the calculations of URCP and SPECTRA (Parameters taken from U25 and the storage ring mode 1 of SSRF).

	harmonic number	peak flux density calculated by URCP (10^{17}photons/s/mrad^2/0.1%BW*)	peak flux density calculated by spectra (10^{17}photons/s/mrad^2/0.1%BW)
tapered mode	1	4.19	4.30
(dg=0.1 mm)	5	0.728	0.750
planar mode	1	4.97	5.09
	5	2.24	2.28

∗ BW means bandwidth.

three components of the magnetic field $\boldsymbol{B}$ in Cartesian coordinates are considered, but the value of $\boldsymbol{B}$ only depends on the longitudinal position. VMT is ignored in this case. A typical EPU, which has 45 periods with a period length of 44 mm is selected as a calculating example. We can simply write the on-axis magnetic field as:

$$\begin{aligned} B_y &= B_0 \sin\left(\frac{2\pi}{\lambda_u} z\right), \\ B_y &= B_0 \cos\left(\frac{2\pi}{\lambda_u} z\right), \\ B_z &= 0. \end{aligned} \tag{22}$$

Figure 6 shows the radiation spectra of EPU. In the case of a magnetic field with random errors, both the horizontal and the vertical peak magnetic field contribute a rms error of 0.5% to the ideal values. In both cases, the effect of beam emittance and energy spread is included. Fig. 7 shows the comparison of the results of URCP and SPECTRA in the EPU case. The difference of the results obtained by the two codes is less than 4%. The reason has been explained in the previous section.

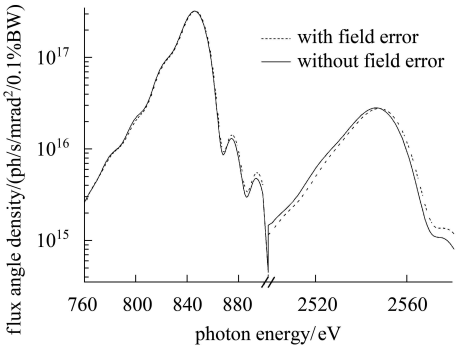

Fig. 6. Radiation spectra of EPU.

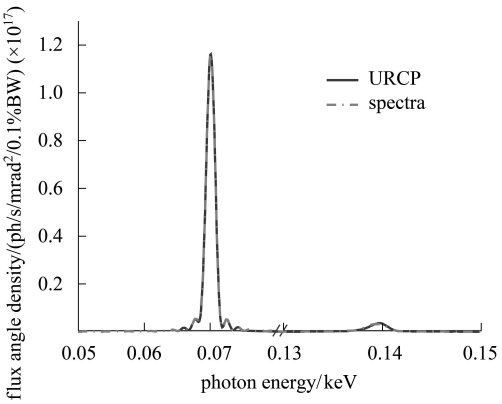

Fig. 7. Radiation spectra calculated by URCP and SPECTRA (EPU under circle polarized mode).

5.3 Undulators with arbitrary magnetic field

Besides the URCP, the other computer codes available at present are based on a quasi-arbitrary magnetic field. This approximation is suitable for the occasion where the electron beam emittance is small or the good field region of the undulator is large enough. However, this approximation is not well suited if the electron beam emittance is large. Then the VMT could seriously affect the undulator radiation and it should be taken into account in a more accurate calculation.

For example, after the coordinate definition given in Fig. 3, the magnetic field intensity distribution of an EPU under linear polarization mode can be expressed as[21, 22]:

$$\begin{aligned} B_x(x,y,z) &= 2B_0\alpha^2\delta xy\cdot\sin(k_u z), \\ B_y(x,y,z) &= B_0[1+\alpha^2\{\delta x^2+(2-\delta)y^2\}\cdot\sin(k_u z), \\ B_z(x,y,z) &= 2B_0\alpha y\cdot\cos(k_u z), \end{aligned} \tag{23}$$

where, $B_0 = 0.7$ T, $k_u = \dfrac{2\pi}{\lambda_u}$, $\alpha = \dfrac{\pi}{\lambda_u}$ and $\delta = 1$ (taking $\lambda_u = 44$ mm) are the parameters of the undulator magnetic structure.

Figure 8 shows the radiation spectra of the first and the fifth harmonic under different electron beam emittances based on the magnetic field pattern mentioned above. The solid lines and the dashed lines show the spectrum with and without the effect of VMT, respectively.

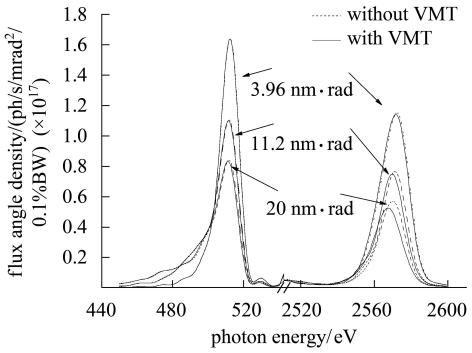

Fig. 8. Flux angle density spectra.

As shown in Fig. 8, if the effect of VMT is taken into account, the peak flux density decreases and the peak position shifts to the low energy side. From Table 3, we can find that for increasing electron beam emittance the effect of VMT on the radiation intensity becomes more serious. The decrease of the radiation intensity could be about 8% in the 5th harmonic. So, considering the effect of VMT will improve the accuracy of the undulator radiation calculation.

6 Comparisons with other codes

We have make the comparisons of XOP and SPECTRA with URCP. XOP is based on an analytic

Table 3. Peak flux density under different emittances.

harmonic number	natural emittance/ (nm·rad)	peak flux density (with VMT) (10^{17}photons/s/mrad^2/0.1%BW)	peak flux density (without VMT) (10^{17}photons/s/mrad^2/0.1%BW)	ratio
1	3.9	1.638	1.639	0.999
1	11.2	1.100	1.106	0.995
1	20.0	0.833	0.842	0.989
5	3.9	1.142	1.152	0.991
5	11.2	0.749	0.766	0.979
5	20.0	0.525	0.571	0.920

method. It can only calculate the basic properties of various kinds of undulator sources for ideal electron trajectories (ideal magnetic field and perfect injection)[6]. Both URCP and SPECTRA[8] can calculate undulator radiation from analytic and simulated parameters. SPECTRA can calculate undulator spectra from a quasi-arbitrary magnetic field without VMT. URCP can deal with an arbitrary magnetic field with VMT and extends the scope of calculation significantly.

7 Discussion and conclusion

This paper introduces a computing method and the related program URCP which can calculate most properties of the undulator radiation in arbitrary 3D magnetic field cases. A comparison shows that the calculating precision of the URCP is at the same level with other computing codes for magnetic fields without VMT. But the URCP can be adapted to more complicated magnetic fields and give more practical and accurate calculation results with large electron emittance or off-axis radiation, by taking into account the effect of VMT. URCP will be helpful for the design of novel undulators and can be applied to more general cases.

URCP applies a Monte Carlo method to deal with the effect of electron bunches. It is somewhat time consuming, however, the calculation speed can be improved further by optimizing the calculation method in the future.

In conclusion, the development of the numerical method and the computer program URCP has extended the capability of calculating undulator radiation spectra. It will be a useful tool for studying the characteristics of undulator radiation and for the design, optimization and test of undulators with better accuracy. So far the experimental measurements for both, radiation spectra and magnetic fields of undulators, were only done in rare cases. Accurate experimental data are still needed fully demonstrate the accuracy of the calculations, which may help to pave a way to the delicate usage of undulator radiation spectra in the future.

The authors thank Prof. Zhou Qiao-gen of SSRF for reading this paper and for the helpful discussion. The authors thank Dr. Chen Nian of SSRF for the helpful discussion. The authors thank also the SSRF staffs at macromolecular crystallography beamline and soft X-ray spectromicroscopy beamline for providing the undulator parameters used in the calculation.

References

1 MA L D, YAN F J. Introduction to Synchrotron Radiation Applications. Shanghai: Fudan University Press, 2001, 30 (in Chinese)
2 Walker R P. Insertion Devices: Undulators and Wigglers. CERN, 1998, **98-04**: 129
3 Takashi Tanaka, Hideo Kitamura. J. Synchrotron Rad., 2001, **8**: 1221
4 Sanchez del Rio Dejus M R J. SPIE Proceedings, 1998, **3448**: 340
5 Ilinski P, Dejus R J, Gluskun E, Morrison T I. SPIE Proceedings, 1996, **2856**: 15
6 Walker R P, Diviacco B. Rev. Sci. Instrum., 1992, **63**(1): 392
7 Boyanov B I, Bunker G, Lee J M, Morrison T I. Nucl. Instrum. Methods A, 1994, **339**: 596
8 Chubar O, Elleaume P. Proc. of the EPAC98 Conference. Institute of Physics Publishing, Bristol, BSL, GBE, UK: 1998, 1177—1179
9 WANG C, XIAN D. Nucl. Instrum. Methods A, 1990, **288**: 649
10 LIU J Y, XU H L, HE D H. Chinese Journal of Lasers A, 1999, **26**(5): 400 (in Chinese)
11 DIAO C Z, LIU J Y, HE D H, JIA Q K, XU H L. Journal of University of Science and Technology of China, 1999, **29**(1): 60 (in Chinese)
12 YANG Z H, WANG Y Z. High Power Laser and Particle Beams, 1999, **11**(5): 575 (in Chinese)
13 ZHOU Q G, DAI Z M, XU H J. HEP & NP, 2004, **28**(7): 785 (in Chinese)
14 CHEN N, ZHANG P F, HE Duo-Hui et al. Nuclear Science and Techniques, 2005, **28**(4): 258 (in Chinese)
15 Jackson J D. Classical Electrodynamics. New York: Wiley, 1975
16 YAN W P, SUN Z Z, WU H W, WEN Z C. Calculation Method and Practice. Nanjing: Southeast University Press, 2000, 148 (in Chinese)
17 Dejus R J. Nucl. Instrum. Methods A, 1994, **347**: 61
18 WANG Chun-Xi. Proc. SPIE, 1993, **2013**: 126
19 Diviacco B, Walker R P. Nucl. Instrum. Methods A, 1996, **368**: 522
20 Elleaume P. Nucl. Instrum. Methods A, 2000, **455**: 503
21 Dattoli G, Renieri A, Torre A. Lectures on FEL and Related Topics. Singapore: World Scientific, 1993
22 Blewett J P, Chasman R. J.Appl. Phys., 1997, **48**: 2692